UDC 666.97-977 : 539.217.1

Pore pressure in heated concrete walls: theoretical prediction

Zdeněk P. Bažant PhD, SE* and Werapol Thonguthai PhD†

NORTHWESTERN UNIVERSITY

SYNOPSIS

Pore-water pressures in concrete can be calculated by a previously developed theory which is based on thermodynamic properties of water and takes into account the huge changes in permeability and sorption isotherm with temperature, as well as the changes of pore space due to temperature and pressure. After reviewing the theory, finite-element solutions are compared with weight-loss tests of Chapman and England, and theoretical predictions are made for rapid heating of thick walls, either sealed or unsealed. A two-dimensional axisymmetric finite-element solution is developed to analyse the effect of a hot spot on the wall. The pore-pressure peaks are found to be much higher than for slow heating (25 atm versus 8 atm), and still about 50% higher when the heating is confined to a hot spot. The moisture movement in regions where the pressure gradient is opposite to the temperature gradient is found to be rather irregular and to exhibit oscillations. The theory predicts the phenomenon of 'moisture clog' suggested by Harmathy on the basis of tests.

Notation

a	= permeability (m/s)
B_W, B_T	= surface emissivity for moisture and heat
b	= heat conductivity
C, C_a, C_w	= isobaric heat capacities of concrete, of absorbed water and of capillary water
g	= gravity acceleration
$\mathbf{J}$	= moisture flux vector
h	= $p/p_{sat}(T)$ = relative vapour pressure in the pores
p, p_{sat}	= pore pressure and its saturation value
$\mathbf{q}$	= heat flux vector
T	= temperature
t	= time
v	= specific volume of water
w	= specific water content of concrete
w_d	= water liberated by dehydration (per m^3)
w_1	= saturation water content of concrete
ρ	= mass density
ρ_0	= 1 g/cm^3

*Professor of Civil Engineering, Northwestern University, Evanston, Illinois 60201, USA.
†Postdoctoral Research Associate, Northwestern University, now Structural Engineer, Gibbs & Hill, Inc., New York, USA.

Introduction

Heating of concrete may produce a significant build-up of pore-water pressure. Thus, rational prediction of the response of concrete to heating requires calculation of moisture transfer. Problems of this type appear in evaluating the safety of primary and secondary nuclear concrete vessels and containments in hypothetical core-disruptive accidents. The theory of the fire resistance of concrete building structures and the design of various industrial vessels (e.g. for coal liquefaction) could also greatly benefit from moisture-transfer calculations.

Although the fire response of concrete structures has been investigated for a long time[1–10], experimental studies of material behaviour above 100°C are relatively recent[1, 4–7, 11–16]. A rational physical mathematical model for the pore pressure build-up and moisture movement in heated concrete was in general formulated in 1975[17] and the detailed theory has been developed in a recent work[18]. The purpose of this paper is to report some further results of the investigations of this problem at Northwestern University, including additional comparisons with test data, estimation of pore pressure caused by a heat shock in a massive wall, and development of a two-dimensional finite-element solution for moisture transfer in heated concrete.

Review of basic theory

First it is necessary to summarize the basic theory set forth in the previous work[18]. The general approach to the coupled moisture and heat transfer in porous solids, as known from irreversible thermodynamics, is to write the vector of the mass flux of moisture, **J**, and the heat flux vector, **q**, as a linear combination of the gradients of pore-water content w and of temperature T[19–21]. This linear relation is given by a square (2 × 2) coefficient matrix, whose off-diagonal coefficients represent cross effects (such as the Soret flux of moisture and the Dufour flux of heat). Studies of test data[18] have, however, indicated that these complete transfer relations are not requisite for modelling concrete and that simplified transfer relations are possible if w is replaced by pore pressure p as the driving force of mass transfer; i.e.

$$\mathbf{J} = -\frac{a}{g}\,\text{grad}\,p;\quad \mathbf{q} = -b\ \text{grad}\,T \quad \ldots\ldots(1a, b)$$

in which a = permeability (of dimension m/s), b = heat conductivity, and g = gravity acceleration, introduced strictly for dimensional convenience.

Obviously equation 1a is the same as Darcy's law. This law is normally limited to saturated porous materials but, on the basis of studies of test data, it appeared that equation 1a may be extended to non-saturated concrete, provided that p is interpreted as the pressure of vapour rather than the pressure of liquid (capillary) water in the pores of heated non-saturated concrete[22–24]. Compared with w or other possible choices for the variable to represent the driving force of moisture transfer, the choice of p is more convenient because it allows the elimination of grad T from the equation for **J**. It should be noted, though, that a certain thermal moisture flux (the Soret flux) is included in equation 1a nonetheless. This is because

$$\text{grad}\,p = (\partial\partial w/\partial p)\,\text{grad}\,p + (\partial w/\partial T)\,\text{grad}\,T$$

which follows by differentiating the sorption relation $w = w(p, T)$.

Water which is chemically bound in hydrated cement becomes free and is released into the pores as the concrete is heated. This must be reflected in the condition of conservation of mass:

$$\frac{\partial w}{\partial t} = -\,\text{div}\,\mathbf{J} + \frac{\partial w_d}{\partial t} \quad \ldots\ldots\ldots(2)$$

in which w represents the free water content, i.e. the mass of all free (not chemically bound) water per m³ of concrete, and w_d denotes the mass of free water that has been released into the pores by dehydration (liberation of chemically bound water). At temperatures below 100°C, the symbol w_d may be used to represent the reverse phenomenon, i.e. the loss of free water caused by hydration, in which case the increments of w_d are negative. Inclusion of w_d in equation 2 is essential and has a major effect in calculations.

The condition of heat balance may be written as

$$\rho C\frac{\partial T}{\partial t} - C_a\frac{\partial w}{\partial t} - C_w\mathbf{J}\cdot\,\text{grad}\,T = -\,\text{div}\,\mathbf{q} \quad \ldots(3)$$

in which ρ and C = mass density and isobaric heat capacity of concrete (per kg of concrete) including its chemically combined water but excluding its free water; C_a = heat capacity of free water plus the heat of adsorption of adsorbed water layers on pore walls; C_w = isobaric heat capacity of bulk (liquid) water. The term $C_w\mathbf{J}\cdot\,\text{grad}\,T$ represents heat convection due to movement of water[20, 21]; normally this term is negligible, but in rapid heating, as in a reactor accident, this might not be true. The heat capacity terms of equation 14 may be further expressed as

$$\rho C\frac{\partial T}{\partial t} = \rho_s C_s\frac{\partial T}{\partial t} - C_d\frac{\partial w_d}{\partial t};$$

$$C_a\frac{\partial w}{\partial t} = \frac{\partial}{\partial t}(w_c H) - C_{ad}\frac{\partial w_{ad}}{\partial t} \quad \ldots\ldots(4a, b)$$

in which ρ_s and C_s = mass density and heat capacity of solid microstructure excluding hydrate water (per m³ of concrete); C_d = heat of dehydration, C_{ad} = heat of adsorption on pore walls; w_c = amount of capillary water (per m³ of concrete) = $w - w_{ad}$; w_{ad} = amount of water adsorbed on pore walls; and $H = H(\rho, T)$ = enthalpy of water. Further complications stem from heat capacity C_s, which includes the heat of chemical conversion of various components of concrete during heating. The heat of vaporization of water does not figure explicitly, but it may be included under $\partial(w_c H)/\partial t$.

The above complex picture notwithstanding, it seems that the distinction between various terms contributing to the heat capacity is not too important for the development of pore pressure. Thus, as an approximation, it is possible to neglect C_a and consider C approximately as a fixed function of temperature.

The boundary conditions for the heat and moisture transfer at the surface are

$$\mathbf{n}\cdot\mathbf{J} = B_w(p_b - p_{en});$$
$$\mathbf{n}\cdot\mathbf{q} = B_T(T_b - T_{en}) + C_w\mathbf{n}\cdot\mathbf{J} \quad \ldots\ldots(5a, b)$$

where **n** is the unit outward normal of the surface; p_{en} and T_{en} are the partial pressure p and temperature of the adjacent environment; and p_b and T_b = the values of p and T just under the surface of concrete. Term $C_w\mathbf{n}\cdot\mathbf{J}$ represents the heat loss due to the latent heat of moisture vaporization at the surface. The special case of a perfectly sealed or perfectly insulated surface is obtained as $B_w \to 0$ or $B_T \to 0$, respectively, and the special case of perfect moisture or heat transmission is obtained as $B_w \to \infty$ or $B_T \to \infty$.

Studies of experimental data have indicated that

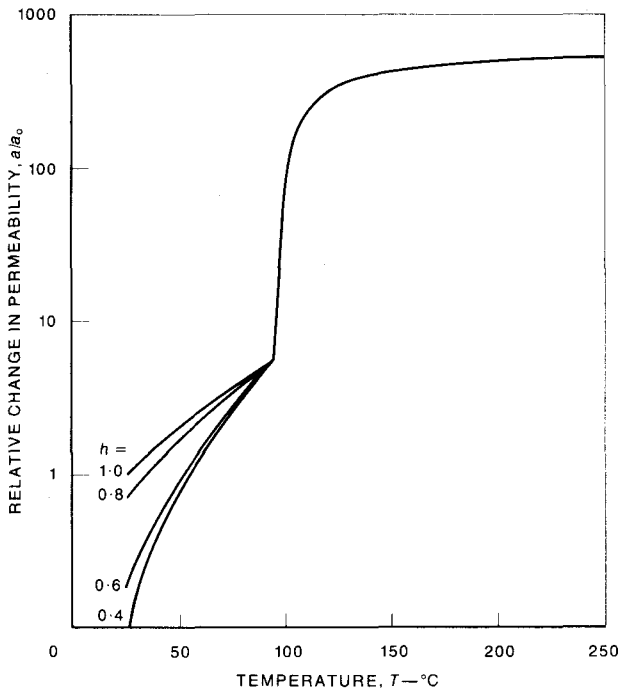

Figure 1: Relative change in permeability with temperature for various values of h.

permeability, a, varies tremendously with temperature. This has profound effects upon the development of pore pressure. The following equation, graphically represented in Figure 1, has been found[18] to give reasonable fits of test data:

$$\text{for } T \leq 95°C: \; a = a_0 f_1(h) f_2(T);$$
$$\text{for } T > 95°C: \; a = a_0' f_3(T) \quad \ldots\ldots (6a, b)$$

where $a_0' = a_0 f_2$ (95°C), a_0 = reference permeability at 25°C, and[22–24]

$$\text{for } h \leq 1: \; f_1(h) = \alpha_T + \frac{1 - \alpha_T}{1 + [4(1-h)]^4}$$
$$\text{for } h > 1: \; f_1(h) = 1 \quad \ldots\ldots\ldots\ldots (7a, b)$$

in which $h = p/p_{sat}(T)$, $p_{sat}(T)$ = saturation vapour pressure, α_T = 0·05 at 25°C and 1·0 at 95°C, whilst between 25°C and 95°C α_T varies roughly linearly, and

$$f_2(T) = \exp\left[\frac{Q}{R}\left(\frac{1}{T_{abs_0}} - \frac{1}{T_{abs}}\right)\right] \quad (\text{for } T \leq 95°C) \quad \ldots\ldots\ldots (8)$$

in which T_{abs} is the absolute temperature, Q = activation energy of low temperature moisture diffusion[22–24], R = gas constant;

$$f_3(T) = \exp\left(\frac{T - 95}{0{\cdot}881 + 0{\cdot}214(T - 95)}\right)$$
$$(\text{for } T > 95°C) \quad \ldots\ldots\ldots\ldots\ldots\ldots\ldots (9)$$

in which T = temperature in °C.

Function $f_2(T)$ implies that the moisture transfer below 95°C is governed by activation energy. This is logical because there are good reasons[22, 18] to believe that moisture transfer is controlled by migration of water molecules along adsorbed water layers in cement gel. Function $f_1(h)$ also reflects this mechanism, as it indicates a decrease in the rate of migration with decreasing thickness of the adsorbed layers. Function $f_3(T)$ represents an upward jump of permeability by two orders of magnitude (about 200 times) when passing from 95° to 105°C, which represents one major finding of the previous work[18]. This jump, which explains the well-known fact that above 100°C concrete can be dried much faster than concrete at normal temperatures, was reported in 1977[25]; a jump of 100 times was at the same time independently observed by Chapman and England[14].

A new hypothesis has been advanced to give a physical explanation of the permeability jump at 100°C that is consistent with the hypothesis of adsorbed water migration at normal temperature[18]. The rate of moisture transfer at ordinary temperature must be controlled by narrow 'necks' on the transfer passages of smallest resistance through the material. These necks are of gel-pore dimensions, below about 10 molecules in thickness, so that water can pass through them only in adsorbed state, but not as vapour or in the liquid state which prevails along the rest of the passage. It would be hard to explain the large increase in permeability by an increase in adsorbed water mobility. As a more logical explanation, it was hypothesized[18] that upon heating beyond 95°C the necks greatly widen, as part of a smoothing process of the rough solid surfaces. Evaporation of adsorbed water from the neck segments may also contribute. If it is assumed that the neck segments of the passage are relatively very short and sparsely spaced along the passage, the assumed large increase in the neck width can be reconciled with the fact that the increase in the total pore volume upon heating is relatively modest and the pore size distribution does not change much. After the narrow necks have been lost ($T > 105°C$), the moisture transfer must be governed chiefly by the viscosity of the steam, which varies only mildly as temperature increases further. This is reflected in function $f_3(T)$. Moreover, when viscosity governs, permeability can no longer depend upon pore pressure, and this is reflected by setting $\alpha = 1$ for $T > 95°C$.

The variation of the pore space that is available to capillary (liquid) water at pressures beyond the saturation pressure is another property of major importance. Obviously, the well-known thermodynamic properties of water (as given, for example, by ASME Steam Tables) must be applicable to capillary water. This would lead, however, to blatantly incorrect results if the pore space were assumed to be constant

and concrete were considered to be fully saturated before heating. One would then obtain pore pressures in excess of 10 000 atm upon heating to 250°C, whereas the highest pore pressure ever measured in heated concrete is about 8 atm. The fact that concrete often does not crack upon heating also implies that the pore pressure is relatively modest.

Consequently, the pore volume n available to capillary water must be assumed to increase significantly with both temperature and pore pressure[18]. The following relations have been found to give a reasonable fit to test data[18]:

$$\text{for } h \geq 1{\cdot}04: \quad n = \left(n_0 + \frac{w_d(T) - w_{d_0}}{\rho_0}\right) P(h)$$

$$w = (1 + 3\epsilon^v)\,\frac{n}{v} \qquad \ldots\ldots\ldots\ldots (10)$$

where $P(h) = 1 + 0{\cdot}12(h - 1{\cdot}04)$. Here n = capillary porosity (i.e. pore space available to capillary water within 1 m³ of concrete), $v = v(T,p)$ = specific volume of water, which depends upon T and p as given by the thermodynamic tables for water, ϵ^v = volumetric (or mean) strain of concrete, $\rho_0 = 1$ g/cm³, $w_d(T) - w_{d_0}$ = amount of free water released into the pores by dehydration = decrease of weight of chemically bound water from $T_0 = 25$°C to T, and n_0 = capillary porosity at 25°C. The sorption isotherms of saturated concrete based on equation 10 are exhibited in Figure 2[18].

The relationship of pore pressure, water content and temperature must further be given for unsaturated concrete (which can exist, of course, only below the critical point of water, 374°C). Assuming that pore geometry does not change and considering the Kelvin relation for capillary pressure and the Laplace equation for capillary meniscus, one would deduce that $w \sim h^{1/m(T)}$.[18] The pore geometry is, of course, not constant. However, lacking a more sophisticated theory, one can assume that a relationship of the same form holds even for pores of changing geometry, but with different coefficients, determined so as to give the best fit of test data. In this manner it has been found[18] that

$$\text{for } h \leq 0{\cdot}96: \quad \frac{w}{c} = \left(\frac{w_1}{c} h\right)^{1/m(T)}$$

$$m(T) = 1{\cdot}04 - \frac{T'}{22{\cdot}3 + T'}$$

$$T' = \left(\frac{T + 10}{T_0 + 10}\right)^2 \qquad \ldots\ldots\ldots\ldots (11$$

in which c = mass of anhydrous cement per m³ of concrete, w_1 = saturation water content at 25°C.

Equation 10 is restricted to $h \geq 1{\cdot}04$ and equation 11 is restricted to $h \leq 0{\cdot}96$. This leaves room for a transition region near $h = 1{\cdot}0$. A smooth transition is required between the saturated and non-saturated

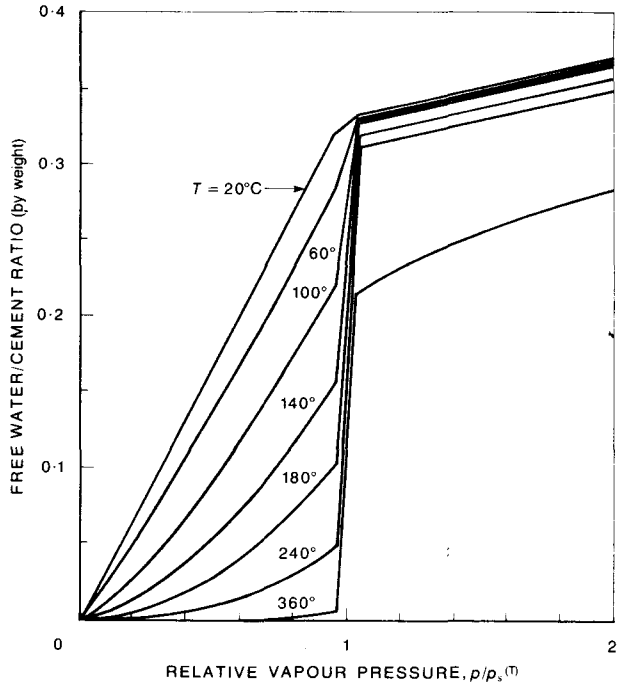

Figure 2: Relation between free water/cement ratio and relative vapour pressure at various temperatures. Concrete density = 2300 kg/m³, cement content = 300 kg/m³, free water content, w = 100 kg/m³.

regimes, as has been noticed when analysing test data. The transition has been assumed as straight lines connecting the values of w at $h = 0{\cdot}96$ and $1{\cdot}04$ at the same T. The complete isotherms as given by equations 10 and 11 are shown in Figure 2.

Further, less important, effects which ought to be included in prediction of pore pressure are the acceleration of ageing due to hydration at elevated temperatures below 100°C. This is an effect that is opposite to dehydration w_d. It causes a significant drop in permeability; approximately[18], $a_0 = a_1 10^x$ where $x = \sqrt{a_2/t_e}$, a_2 = constant and t_e = equivalent hydration period (maturity).

Initial-boundary value problem

Substituting $w = w(T,p)$ along with equations 1a and b into equations 2 and 3, we obtain the field equations:

$$\frac{\partial}{\partial r}\left(a\frac{\partial p}{\partial r}\right) + \frac{a}{r}\frac{\partial p}{\partial r} + \frac{\partial}{\partial z}\left(a\frac{\partial p}{\partial z}\right) + A_1\frac{\partial p}{\partial t} + A_2\frac{\partial T}{\partial t} + A_3 = 0 \quad \ldots(12)$$

$$\frac{\partial}{\partial r}\left(b\frac{\partial T}{\partial r}\right) + \frac{b}{r}\frac{\partial T}{\partial r} + \frac{\partial}{\partial z}\left(b\frac{\partial T}{\partial z}\right) + A_4\frac{\partial T}{\partial r} + A_5\frac{\partial T}{\partial z} + A_6\frac{\partial T}{\partial t} + A_7\frac{\partial p}{\partial t} = 0 \quad \ldots\ldots\ldots\ldots (13)$$

in which

$$A_1 = -\frac{\partial w}{\partial p}, A_2 = -\frac{\partial w}{\partial T}, A_3 = \frac{\partial w_d}{\partial t} \quad \ldots\ldots(14)$$

$$A_4 = -aC_w\frac{\partial p}{\partial r}, A_5 = -aC_w\frac{\partial p}{\partial z}$$

$$A_6 = C_a\frac{\partial w}{\partial T} - \rho C, A_7 = C_a\frac{\partial w}{\partial p} \quad \ldots\ldots(15)$$

and r, z are the rectangular co-ordinates in an axial plane, z being the axis of symmetry. Note that functions of p, w and T which would make equations 13 and 14 non-linear are put into the coefficients so as to lend equations 12 and 13 a linear form. The values of these coefficients have to be obtained by iterations.

Using equations 1a and b, we may also bring the boundary conditions in equations 5a and b to the form:

$$a\left(\frac{\partial p}{\partial r} + \frac{\partial p}{\partial z}\right) + B_w(p_b - p_{en}) = 0 \quad \ldots\ldots(16)$$

$$b\left(\frac{\partial T}{\partial r} + \frac{\partial T}{\partial z}\right) - C_w a\left(\frac{\partial p}{\partial r} + \frac{\partial p}{\partial z}\right) + B_T(T_b - T_{en}) \quad \ldots\ldots(17)$$

Equations 12 and 13, together with the boundary conditions in equations 16 and 17, define an axisymmetric two-dimensional initial-boundary value problem, which is essentially of diffusion type.

Experimental calibration and prediction of moisture loss

Although numerous test data have been accumulated in fire research, there seem to exist no direct measurements of sorption isotherms at elevated temperatures or at pressures beyond the saturation point. In fact, even transient measurements are extremely scant. It is just for this reason that physical reasoning and theoretical approach are necessary. The few pertinent test data that were available[4,13–16], including measured pressure and temperature distributions at various times, together with drying tests of heated unsealed concrete cylinders carried out at Northwestern University[18], did allow calibration of the theory nonetheless; see reference 18*. For the fitting of test data, a finite-element solution of the equation system (equations 1 to 11), one-dimensional and axisymmetric in space, has been developed in reference 18.

After this work had been completed, further relevant test results were published by Chapman and England[14]. They measured pore-pressure and water-loss histories at various places within a concrete cylinder that was sealed and thermally insulated, except for being vented at one end and heated to a certain temperature at the other end; see the broken lines in Figure 2 and, for details, reference 14. These tests, which are an extension of those fitted previously[18], offer an opportunity to check the theory. Therefore, theoretical predictions for the case tested have been run with the finite-element program described in reference 18. The results are shown by solid lines in Figure 3, whereas the Chapman and England's data are plotted by broken lines. Furthermore, their measured weight losses for various specimens are compared with our predictions in Table 1.

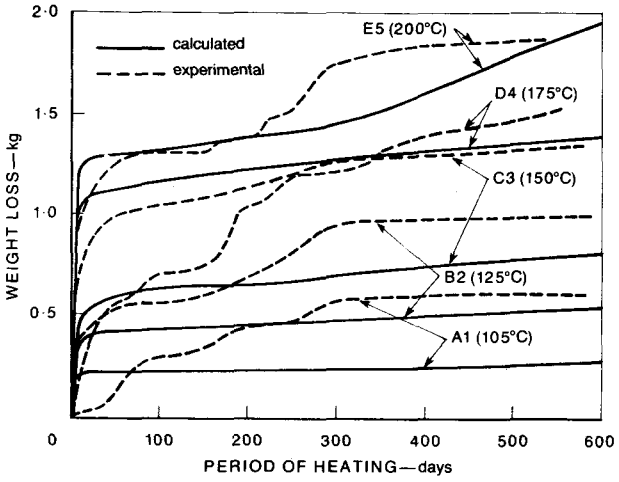

Figure 3: Relation between weight loss and time of heating, calculated and from the test data of Chapman and England[14]. Thermal conductivity = 1·67 J/m s °C, permeability = 2·5 × 10^{-11} m/s, saturation water content = 100 kg/m³.

*Note these corrigenda in reference 18: on p. 1077, in line 14, replace 100·0 by 1·67, and in line 25 replace 20·9 by 0·35.

TABLE 1: **Comparison of calculated weight losses with measurements of Chapman and England[14].**

Specimen No.	Cylinder length (m)	Age (days)	Duration of heating (days)	Temperature at hot end (°C)	Temperature at cold end (°C)	Weight of mix water (kg)	Measured weight loss (kg)	Theoretical weight loss (kg)
A1	1·5	181	582	105	41	5·13	0·63	0·28
B2	1·5	182	588	125	46	5·13	1·05	0·58
C3	1·5	196	573	150	50	5·10	1·42	0·83
D4	1·5	195	554	175	55	5·22	1·61	1·46
E5	1·5	216	531	200	76	5·17	1·98	2·00
P16	3·0	239	697	150	58	9·30	3·20	1·77
Q17	3·0	224	512	125	52	10·2	2·00	1·11
R18	3·0	208	525	105	44	10·2	1·13	0·53
S19	3·0	317	401	200	76	10·3	3·71	3·27
T20	3·0	316	401	175	70	10·3	3·33	2·39

Since this is not a fit but a prediction, the agreement is relatively satisfactory. Moreoever, it should be noted that part of the difference is due to considering the problem as one-dimensional. In reality, heat is conducted in the axial direction not only by concrete, but also by the sealing metallic jacket. This would tend to increase the moisture loss, and indeed the experimental values in Figure 3 are generally higher than the calculated ones.

Pore pressure and moisture clog due to rapid heating

For the failure analysis of concrete reactor vessels in accidents or of structures subjected to fire, the

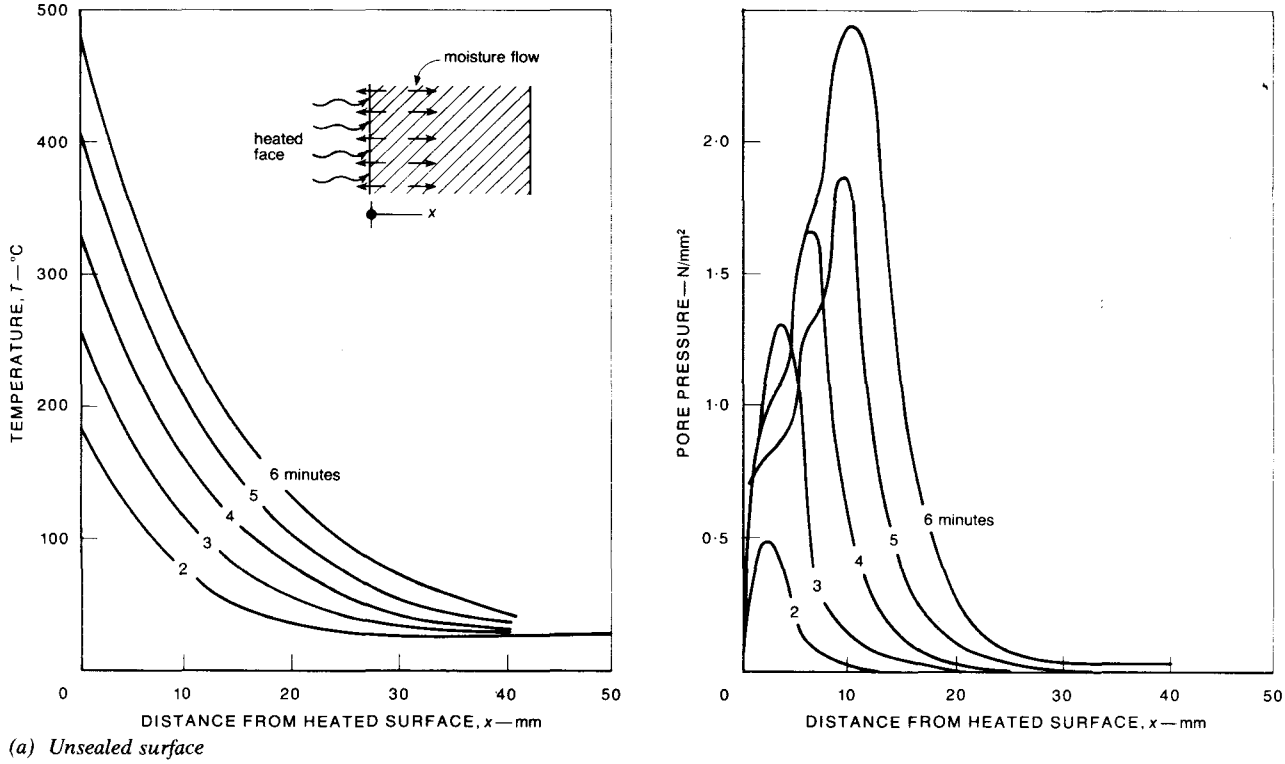

(a) Unsealed surface

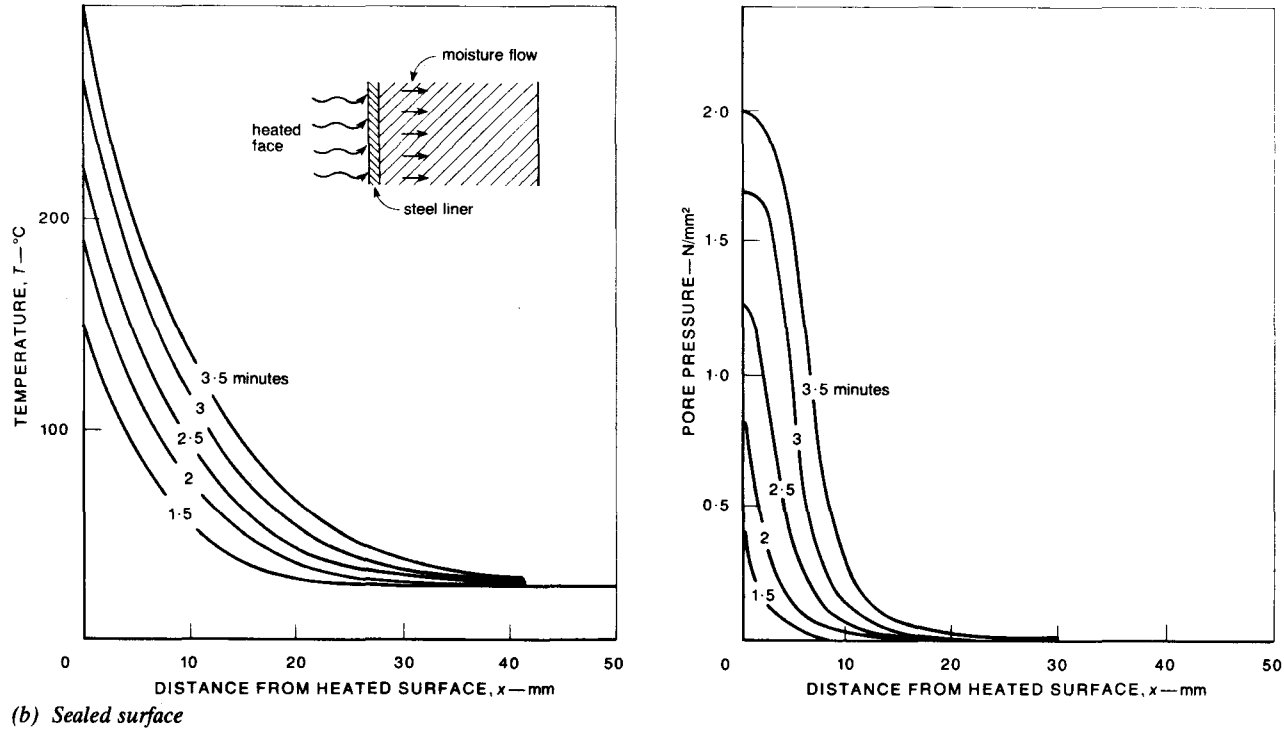

(b) Sealed surface

Figure 4: Relation between temperature and pore pressure, and distance, x, from heated surface. Thermal conductivity = 1·67 J/m s °C, permeability = 10^{-12} m/s, saturation water content = 100 kg/m³, water/cement ratio = 0·50, unit mass of concrete = 2400 kg/m³, rate of heating = 80 °C/min.

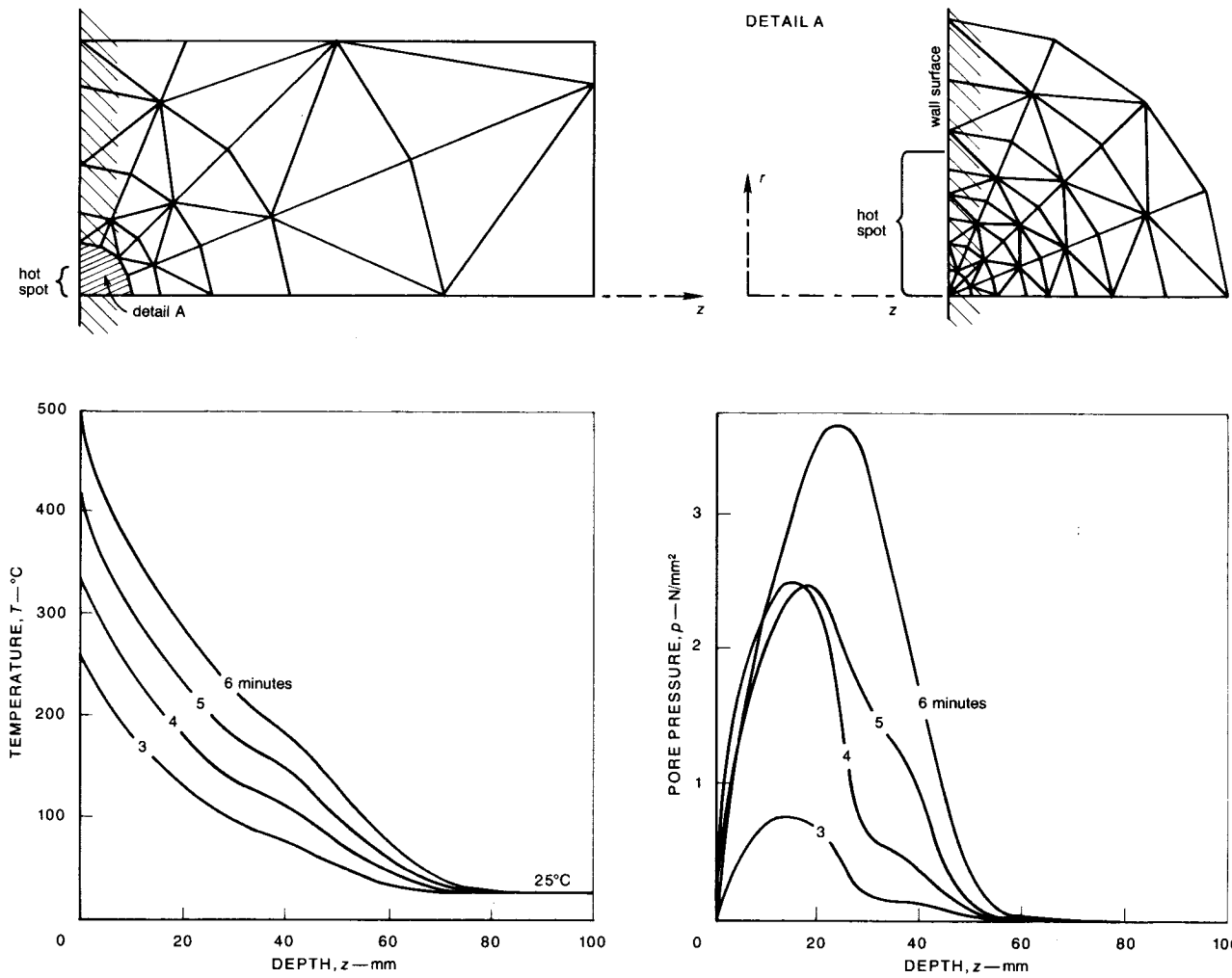

Figure 5: Relation between temperature and pore pressure, and distance, z, from hot spot for various periods of heating (calculated).

question of possible explosive spalling is of great concern. There are two possible causes of this phenomenon: (a) instability (buckling) of a surface layer in a hot region, in which a compressive normal stress parallel to the surface of a wall or slab is induced, owing to the restraint provided by the surrounding non-heated region or structure, and (b) tension in the solid microstructures that is produced by the pore pressure. Lacking calculations, it has not been possible to say which cause is the major one, or under which conditions. The present theory now allows us, however, to examine at least cause (b), a rise in pore pressure due to rapid heating ('thermal shock').

By using the computer program described in reference 18, calculations have been made for a concrete wall of thickness over 200 mm, rapidly heated at one face ($x = 0$) in such a manner that the temperature of the face rises linearly at the rate of 80°C/min. The assumed properties of the concrete are given in Figure 4, where the curves indicate the calculated distributions of temperature and pore pressure at various times after the start of heating. Calculations are made for two moisture boundary conditions: unsealed heated surface (with $p \approx 1$ kN/m²), and sealed heated surface (e.g. with a steel liner as in a reactor vessel).

Although the temperature distributions do not exhibit anything unusual, the calculated pore pressure curves (Figure 4) are quite interesting. First of all the pressure peaks are much higher than those for slow heating[18]. Furthermore, although the pressure peaks in the sealed wall are higher than in the unsealed one, they are not much higher. The pressure penetration into the unsealed wall is at some points even faster than into the sealed wall. For example, at depth $x = 5$ mm and time 3 min, $p = 1{\cdot}20$ N/mm² for the unsealed wall and 0·85 N/mm² for the sealed wall. The rising branches of pressure in the unsealed wall show a rather erratic trend and the locations of the steep pressure gradient tend to oscillate back and forth. The calculation of the rising segments of pressure curves turned out to be extremely sensitive to the time step and element size and required these to be taken rather small.

The complicated and at first unexpected behaviour of pore pressure is no doubt caused by the competing influences that the pressure and temperature gradients exert upon moisture movement. The former tends to drive water towards the unsealed but heated surface, whereas the latter tends to drive water into the wall, away from the heated surface. The first tendency prevails near the surface where concrete is already almost dry, and also near the heating front. In the middle portion, an extremely steep downward slope of pressure curve develops (Figure 4), where the tendency is for water to be pushed into the specimen, creating an oversaturated zone. This is precisely what Harmathy[26] intuitively hypothesized on the basis of his tests, in which he did actually observe the oversaturated zone and noted that its formation must impede moisture escape from the wall. He aptly called it 'moisture clog'. It is rewarding to find that our equations predict the moisture clog theoretically.

As for the magnitudes of pressure peaks, they are quite significant in comparison with the tensile strength at high temperature, and they can in fact cause tensile failure, i.e. cause a layer of concrete to spall.

The hot-spot problem

In practical problems, the heating may often be non-uniform along the wall surface, an extreme case of which is the 'hot spot'. Assuming the hot spot to be circular, the problem can be solved by a two-dimensional axisymmetric finite-element program (see Appendix). The finite-element grid used is shown in Figure 5. All grid boundaries have been considered at $p \approx 0$ ($p = 1$ kN/m^2), and the heating, again at the rate of 80°C/min, was applied within the surface radius shown. Concrete properties were considered the same as in Figure 4.

The results of finite-element calculations are shown in Figure 5. Compared to the previous one-dimensional heated wall problem (Figure 4), we see a similar pattern of pressure. However, the pressure peak is about 50% higher. This is at first surprising because the heated region occupies a smaller portion of the body and there is more cold concrete into which water can be driven. The higher pressure peak is no doubt caused by the fact that the region of high permeability, which occurs in the heated region, occupies only a portion of the surface so that water has a narrower passage for escaping. The trend of pressure change is even more erratic than before; e.g. the pressure peak at 5 min is less than at 6 min and it generally goes up in jumps (giving an oscillating time curve).

Conclusions

(1) On the basis of the previously developed and experimentally calibrated theory[18], moisture loss is predicted for a recently reported test by Chapman and England[14]. The predictions are in relatively satisfactory agreement with their measurements.
(2) For rapid uniform heating of one face of a thick wall (thermal shock), the calculated pore pressure peaks are much higher than for slow heating (e.g. 25 atm as against 8 atm).
(3) For a rapidly heated small hot spot on the surface of a thick wall, the calculated pore pressure peaks are still higher, by about 50%.
(4) In the region where the pressure gradient is opposite to the temperature gradient, the calculated moisture movement is rather irregular and tends to give oscillations in pore pressure. Convergence of the numerical solution in this region is also difficult to attain.
(5) The theory predicts for a rapidly heated wall the phenomenon of 'moisture clog' which was suggested by Harmathy[26] on the basis of his tests.

ACKNOWLEDGEMENT

Support under the U.S. National Science Foundation Grant No. ENG-14848-A01 to Northwestern University is gratefully acknowledged. The first author is also grateful for partial support under the Guggenheim Fellowship awarded to him for 1978–79.

REFERENCES

1. BAŽANT, Z. P. Review of literature on high temperature behavior of concrete. pp. 71–142 of the Report. *Evaluation of the structural integrity of LMFBR equipment cell liners – results of preliminary investigations* by W. J. MCAFFEE, W. K. SARTORY, Z. P. BAŽANT and P. A. STANCAMPIANO. Tennessee, Oak Ridge National Laboratory, (Contract W-7405 eng 26), January 1976. Report ORNL-TM-514S. (Available from National Technical Information Service, Springfield, Va.)
2. BECKER, J. M. and BRESLER, B. Reinforced concrete frames in fire environments. *Proceedings of the American Society of Civil Engineers.* Vol. 103, No. ST1. January 1977. pp. 211–224.
3. DOUGILL, J. W. Conditions for instability in restrained concrete panels exposed to fire. *Magazine of Concrete Research.* Vol. 24. 1972. pp. 139–148.
4. ENGLAND, G. L. and ROSS, A. D. Shrinkage, moisture, and pore pressures in heated concrete. *Concrete for nuclear reactors.* Detroit, American Concrete Institute, 1972. Special Publication SP-34. Vol. II. pp. 883–907.
5. FISCHER, R. Über das Verhalten von Zementmortel und Beton bei hoheren Temperaturen. (On the behaviour of cement mortar and concrete at high temperatures.) Berlin, Wilhelm Ernst und Sohn, 1970. Deutscher Ausschuss für Stahlbeton. Heft 216. pp. 61–128.
6. HARMATHY, T. Z. Thermal properties of concrete at elevated temperatures. *ASTM Journal of Materials.* Vol. 5, No. 1. March 1970. pp. 47–74. Reprint: Ottawa, National Research Council of Canada, 1970. DBR Paper No. 426.
7. HARMATHY, T. Z. and ALLEN, L. W. Thermal properties of selected masonry unit concretes. *Journal of the American Concrete Institute. Proceedings* Vol. 70, No. 2. February 1973. pp. 132–144.

8. HUNDT, J. Zur Warme- und Feuchtigkeitsleitung in Beton. (Heat and moisture conduction in concrete.) Berlin, Wilhelm Ernst und Sohn, 1977. Deutscher Ausschuss für Stahlbeton. Heft 280. pp. 21–41.
9. MCDONALD, J. E. *Moisture migration in concrete.* Vicksburg, Miss., U.S. Army Engineers Waterways Experimental Station, Concrete Laboratory, May 1975. Technical Report C-75-1. pp. 36 + Tables + Plates.
10. NEVILLE, A. M. *Properties of concretes.* New York, John Wiley and Sons, 1973. A Halsted Press Book.
11. AL-ALUSI, H. R., BERTERO, V. V. and POLIVKA, M. *Effects of humidity on the time-dependent behavior of concrete under sustained loading.* Berkeley, University of California, January 1972. Report No. UC SCSM 72-2.
12. BERTERO, V. V., BRESLER, B. and POLIVKA, M. Instrumentation and techniques for study of concrete properties at elevated temperatures. *Concrete for nuclear reactors.* Detroit, American Concrete Institute, 1972. Special Publication No. SP-34. Vol. III. pp. 1377–1419.
13. ENGLAND, G. L. and SHARP, T. J. Migration of moisture and pore pressure in heated concrete. *Proceedings, First International Conference on Structural Mechanics in Reactor Technology. Berlin, 1971.* Editor: T. A. JAEGER. Brussels, Commission of European Communities, 1971. pp. 129–143. Paper H2/4.
14. CHAPMAN, D. A. and ENGLAND, G. L. Effects of moisture migration on shrinkage, pore pressure and other concrete properties. *Transactions, Fourth International Conference on Structural Mechanics in Reactor Technology,* San Francisco, August 1977. Editors: B. A. BOLEY and T. A. JAEGER. Brussels, Commission of European Communities, 1971. Paper M5/3.
15. ZHUKOV, V. V. and SHEVCHENKO, V. I. Investigation of causes of possible spalling and failure of heat-resistant concretes at drying, first heating and cooling. In: "Zharostoikie betony" (Heat-resistant concrete). Editor: E. D. NEKRASOV. Moscow, Stroiizdat, 1974. pp. 32–45.
16. ZHUKOV, V. V., ROBSMAN, V. A., SHEVCHENKO, V. I. and CYGANOVA, L. P. Thermophysical analysis of structures of heat-resistant concrete. (Teplofizicheskie Raschety Konstrukcii iz Zharostoikogo Betona na AVM i CVM.) Volgograd, NII ZhB, 1971.
17. BAŽANT, Z. P. Some questions of material inelasticity and failure in the design of concrete structures for nuclear reactors. Transactions, Third International Conference on Reactor Technology. London, September 1975. Editor: T. A. JAEGER. Brussels, Commission of European Communities, 1975. Paper H1/1.
18. BAŽANT, Z. P. and THONGUTHAI, W. Pore pressure and drying of concrete at high temperature. *Proceedings of the American Society of Civil Engineers.* Vol. 104, No. EM5. October 1978. pp. 1059–1079. (For a summary, see BAŽANT, Z. P. Thermal effects, creep and nonlinear response of concrete reactor vessels. *Proceedings 4th Conference on Structural Analysis, Design and Construction of Nuclear Power Plants. Porto Alegre, Brazil, 1978.* pp. 117–130.)
19. DEGROOT, S. R. and MAZUR, P. *Non-equilibrium thermodynamics.* New York, North Holland-Interscience Publishers, 1962.
20. LYKOV, A. V. and MIKHAILOV, YU. A. Theory of energy and mass transfer. (Translated from the Russian.) Englewood Cliffs, N.J., Prentice Hall, 1961.
21. WELTY, J. R., WICKS, C. E. and WILSON, R. E. *Fundamentals of heat and mass transfer.* New York, John Wiley and Sons, 1969.
22. BAŽANT, Z. P. and NAJJAR, L. J. Nonlinear water diffusion in nonsaturated concrete. *Materials and Structures: Research and Testing.* Vol. 5, No. 25. January–February 1972. pp. 3–20.
23. BAŽANT, Z. P. Pore pressure, uplift, and failure analysis of concrete dams. *Proceedings, International Commission of Large Dams Symposium on Criteria and Assumptions for Numerical Analysis of Dams, Swansea, September 1975.* Swansea, University College, 1975. pp. 781–808.
24. BAŽANT, Z. P. Theory of creep and shrinkage in concrete structures: A précis of recent developments. *Mechanics Today.* New York, Pergamon Press, 1975. Vol. 2. pp. 1–93.
25. BAŽANT, Z. P. Material problems in accident analysis of prestressed concrete reactor vessels. *Transactions, Fourth International Conference on Structural Mechanics in Reactor Technology, San Francisco, August 1977.* Editors: T. A. JAEGER and B. A. BOLEY. Brussels, Commission of European Communities, 1977. Vol. E, Paper E6/1.
26. HARMATHY, T. Z. Effect of moisture on the fire endurance of building materials. *Moisture in materials in relation to fire tests.* Philadelphia, ASTM, 1965. Technical Publication No. 385. pp. 74–95.
27. ZIENKIEWICZ, O. C. *The finite element method.* Third edition. London McGraw-Hill Book Co., 1977.

APPENDIX

Axisymmetric two-dimensional finite-element solution

The one-dimensional solution has been developed in reference 18, and the two-dimensional axisymmetric solution that we now briefly outline is analogous. Equations 12 and 13, together with the boundary conditions in equations 16 and 17, may be equivalently expressed by the variational equations:

$$\int \text{LHS (equation 12)}\, \delta p \, dA - \int \text{LHS (equation 16)}\, \delta p \, ds = 0 \quad \ldots\ldots(18)$$

$$\int \text{LHS (equation 13)}\, \delta T \, dA - \int \text{LHS (equation 17)}\, \delta T \, ds = 0 \quad \ldots\ldots(19)$$

which must hold for any admissible variations δp, δT. LHS denotes the left-hand side of the equations; A is the area of the region and s is its boundary curve.

A finite-element solution may be obtained by using a Galerkin-type procedure[27]. To get rid of the second spatial derivatives of p and T, we apply Green's integral theorem (or Gauss theorem) to the area integrals in equations 18 and 19. This happens to cancel derivatives in the boundary integrals. Because the theory cannot be expected to be highly accurate, the finite elements have been chosen simply as constant-gradient triangles having three nodes, for which $p = \sum_i p_i(t) N_i(r,z)$ and $T = \sum_i T_i(t) N_i(r,z)$ where $i = 1,2,3$; p_i and T_i = nodal values of p and T, $N_i(r,z)$ = linear interpolation functions (shape functions) on the triangle. Substituting this into equations 18 and 19, we get a matrix variational equation, and imposing the condition that it must hold for any nodal variations δp_1, δT_1, we obtain

$$\mathbf{K}_1 \dot{\mathbf{p}} + \mathbf{K}_2 \dot{\mathbf{T}} + \mathbf{K}_3 \mathbf{p} + \mathbf{F}_1 = 0; \quad \mathbf{K}_4 \dot{\mathbf{T}} + \mathbf{K}_5 \dot{\mathbf{p}} + \mathbf{K}_6 \mathbf{T} + \mathbf{F}_2 = 0 \quad \ldots\ldots(20)$$

in which $\mathbf{p}$ and $\mathbf{T}$ are the column matrices formed of the nodal values p_1 and T_1 of the entire grid, and $\mathbf{K}_1 \ldots, \mathbf{K}_6$ are square matrices which are obtained by assembling the elemental matrices, the components of which are:

$$K^{el}_{1ij} = A_1 \int_{el} N_i N_j \, dA, \quad K^{el}_{2ij} = A_2 \int_{el} N_i N_j \, dA$$

$$K^{el}_{3ij} = a \int_{el} \left(\frac{1}{r} \frac{\partial N_i}{\partial r} N_j - \frac{\partial N_i}{\partial r} \frac{\partial N_j}{\partial r} \quad \frac{\partial N_i}{\partial z} \frac{\partial N_j}{\partial z} \right) dA$$

$$K^{el}_{4ij} = A_6 \int_{el} N_i N_j \, dA, \quad K^{el}_{5ij} = A_6 \int_{el} N_i N_j \, dA$$

$$K^{el}_{6ij} = K^{el}_{3ij} \frac{b}{a} + \int_{el} \left(A_4 \frac{\partial N_i}{\partial r} N_j + A_5 \frac{\partial N_i}{\partial z} N_j \right) dA \quad \ldots\ldots(21)$$

where subscript el refers to the element area. $\mathbf{F}_1$, $\mathbf{F}_2$ are force matrices which are obtained by assembling the elemental components:

$$F_{1i}^{el} = A_3 \int_{el} N_i \, dA - [B_w(p_i - p_{en})]_{surf}$$

$$F_{2i}^{el} = A_7 \int_{el} N_i \, dA - [B_T(T_i - T_{en})]_{surf} + \left[aC_w \left(\frac{\partial p}{\partial r} + \frac{\partial p}{\partial z} \right) \right]_{surf} \quad \ldots\ldots(22)$$

in which the terms with subscript "surf" are omitted except for boundary nodes. The non-linearity of the problem is reflected in the dependence of coefficients $\mathbf{K}_{1ij}^{el}, \ldots, \mathbf{K}_{6ij}^{el}, \mathbf{F}_1^{el}, \mathbf{F}_2^{el}$ upon nodal unknowns p_i and T_i. In each time step, these coefficients are first evaluated from the values of p_i and T_i at the beginning of the step, and in subsequent iterations of the step they are evaluated from the averages of initial and final values obtained for this step in the previous iteration.

The solution has been programmed for a CDC computer. It can be also used for non-axisymmetric two-dimensional problems, if one considers the entire grid to be extremely far from the axis z.

Contributions discussing the above paper should be in the hands of the Editor not later than 31 December 1979.